

Beam Driven Alfvén Eigenmodes and Fishbones in the Joint European Torus

"This document is intended for publication in the open literature. It is made available on the understanding that it may not be further circulated and extracts may not be published prior to publication of the original, without the consent of the Publications Officer, JET Joint Undertaking, Abingdon, Oxon, OX14 3EA, UK".

"Enquiries about Copyright and reproduction should be addressed to the Publications Officer, JET Joint Undertaking, Abingdon, Oxon, OX14 3EA".

Beam Driven Alfvén Eigenmodes and Fishbones in the Joint European Torus

D Borba¹, B Alper, R Budny², A Fasoli³, R F Heeter²,
W Kerner, S E Sharapov, P Smeulders.

JET Joint Undertaking, Abingdon, Oxfordshire, OX14 3EA,

¹Also at Assoc. EURATOM/IST, Av Rovisto Pais, 1096 Lisbon, Codex, Portugal.

²Also at PPPL, PO Box 451, Princeton, NJ08543, USA.

³CRPP/EPFL, Ass. EURATOM-Confédération Suisse, 1015 Lausanne, Switzerland.

ABSTRACT

Fast particle driven instabilities are investigated at low toroidal field $B_0 \approx 1T$ in Tritium (T), Deuterium (D) and Hydrogen (H) plasmas. T, D, H neutral beams with energies of 160 keV, 140 keV and 110 keV were injected respectively into T, D and H plasmas. The destabilisation of Alfvén Eigenmodes (AE) was observed during injection of tritium beams into a tritium plasma and during the injection of deuterium beams into a deuterium plasma but not during the injection of hydrogen beams into a hydrogen plasma. At high beta $\beta_N = \frac{\beta}{(I_p/B_T a)} > 2.5$ high amplitude fishbones were observed and appeared to correlate with the degradation of confinement.

1. INTRODUCTION

Energetic ions with velocities comparable to the Alfvén velocity $V_A = B_0 / \sqrt{4\pi\rho}$, where B_0 denotes the equilibrium magnetic field and ρ the plasma mass density, can destabilise Alfvén waves in magnetically confined plasmas through the resonant wave-particle interaction [1, 2]. In deuterium-tritium (DT) thermonuclear tokamak reactors the alpha particles, created by fusion reactions with energies around 3.5 MeV, are super-Alfvénic, $V_{alpha} > V_{Alfven}$, and can interact strongly with Alfvén waves during their collisional slowing down process. The destabilisation of Alfvén Eigenmodes (AE) [3] by the fusion-born alpha particles in tokamaks was first theoretically analysed in [4] and experimentally observed on TFTR [5].

The energetic ions produced by auxiliary heating such as neutral beam injection (NBI) or ion cyclotron resonant heating (ICRH) can also destabilise AE [6-9]. In particular, in fusion reactors where injection of high energy $E_j \sim 1$ MeV super-Alfvénic neutral beams are used either for auxiliary heating or current drive, unstable AE can lead to the reduction of the heating and current drive efficiency. The destabilisation of AE by NBI with energies 80-160 keV can be obtained in the present tokamaks only at low values of the toroidal magnetic field, $B_T \leq 1$ T. At low magnetic field the Alfvén velocity is sufficiently small for an effective resonance, $V_{||beam} \approx V_A$, between the wave and the particles. The destabilisation of Toroidicity Induced Alfvén eigenmodes (TAEs) by the NBI-produced energetic ions has been first demonstrated in low magnetic field discharges on TFTR [6] and DIII-D [7].

In TFTR the TAE instability was driven by deuterium NBI with energies of up to 110 keV injected into a deuterium plasma at low magnetic fields (1T) [6]. Reductions in the neutron rate of up to 10% in a single TAE burst were observed, with estimated cumulative beam loss of up to 50% [10]. Similar experiments were carried out in DIII-D [7] using both hydrogen and deuterium NBI in the low magnetic toroidal field (0.7 T - 1 T) deuterium plasmas. The TAE instability was observed during deuterium NBI only and was absent during hydrogen NBI. Up to 50% beam losses were seen correlated with the destabilisation of TAEs. In both experiments on TFTR and DIII-D, TAEs with intermediate toroidal mode number, $n \geq 2$, were destabilised.

The observation of Alfvén instabilities driven by NBI in JET discharges with low toroidal magnetic field is reported in this paper. The experiments were conducted using tritium NBI into tritium plasma, deuterium NBI into deuterium plasma, and hydrogen NBI into hydrogen plasma. This set of experiments further demonstrates the AE excitation by using different techniques in JET such as the excitation of AE using external antennas (the JET saddle-coils and the ICRH beat waves) [11, 12] and the destabilisation of AE by energetic ions accelerated by ICRH [8, 9, 13-16]. In addition, the distribution of NBI-produced ions and the NBI deposition profile are known with higher degree of accuracy than the ICRH tail distributions. Therefore, the destabilisation of AE by the beam passing ions provides a better possibility for testing the theoretical modelling.

The destabilisation of AE was achieved by the injection of T beams with an energy $E_T \approx 160$ keV into a T plasma at a toroidal magnetic field of 0.9 T (pulse #43014) and by the injection of D beams with energy $E_D \approx 140$ keV into a D plasma at a toroidal magnetic field of 0.8 T (pulse #43846, pulse #43847). No evidence of the AE destabilisation was seen in experiments with injection of H beams (energy $E_H \approx 110$ keV, pulses #43452, #43453) into H plasma at low toroidal magnetic field.

In addition to the AE destabilisation, fishbone bursts [17,18] were observed in the low magnetic field discharges and correlated with the degradation of confinement. They appear as a low toroidal mode number ($n=1$) perturbation with frequencies (20-30 kHz) above the plasma rotation frequency and they chirp down during the burst to frequencies close to the plasma rotation (0-30 kHz). Fishbones are associated with the $q=1$ rational surface and have a dominant $n=1, m=1$ mode structure [19,20,21]. In discharges, where the current profile has been modified and the central value of the safety factor is greater than one ($q_0 > 1$), fishbone-like bursts are also observed with a dominant ($n=1, m=2$) mode structure associated with the $q=2$ rational surface [22]. Typically, fishbones appear with low amplitude $\frac{\delta B}{B} < 10^{-3}$, and no degradation of confinement is observed in JET. In discharges with a large fraction of energetic ions, produced either by strong auxiliary heating ($P_{\text{aux}} = P_{\text{icrh}} + P_{\text{nbi}} > 20$ MW) in low density plasmas or low magnetic field auxiliary heated discharges, fishbone bursts can have very large amplitudes $\frac{\delta B}{B} \approx 10^{-2}$. In high beta $\beta_N > 2.5$ plasmas, where the mode structure is expected to be of a global nature due to enhanced poloidal mode coupling, fishbone bursts are associated with the degradation of confinement. Under these conditions drops in both temperature and neutron rate of up to 10% have been associated with fishbone activity [17].

2. EXPERIMENT AND MEASUREMENTS

Experiments using different hydrogen isotopes (hydrogen, deuterium and tritium) plasmas were conducted on JET at a low toroidal magnetic field during the 1997-1998 campaign. The aim of

these experiments was to study the confinement properties of the different species (H,D,T) in X-point divertor plasmas at varying toroidal magnetic fields and plasma currents. In these experiments, the toroidal magnetic field was varied from the usual value for the normal JET high performance operation, $B_T = 3.4$ T, to magnetic field values as low as $B_T = 0.8$ T. The plasma currents (I_p) were chosen so that I_p/B_T was kept to the order of 1 MA/T, in order to ensure a similar safety factor profile (q) for these discharges. Neutral beam auxiliary heating power of up 15 MW was injected into low field (1T), low density ($2-3 \times 10^{19} \text{ m}^{-3}$) and low current (1 MA) plasmas, maximising the drive of AE as shown in Figure 1.

In JET the diagnostics which can measure electromagnetic fluctuations with frequencies in the Alfvén frequency range include the “Mirnov” magnetic probes, density fluctuation

measurements using microwave reflectometry, soft X-ray emission, electron cyclotron emission and visible spectroscopy. The “Mirnov” pick-up coils can detect magnetic fluctuations of the order of $\frac{\delta B}{B} \approx 10^{-7}$ and have a very small noise level. Magnetic fluctuation measurements with a sampling rate of up to 2 MHz, using a toroidal set of 6 Mirnov probes localised in the low field side of the vessel, have been routinely performed during the 1997 campaign. This allowed the detailed study of the Alfvén eigenmode activity in all plasma configurations.

At low toroidal field, such as the field required for the destabilisation of AE using neutral beams ($B_T < 1$ T), the frequency of AE is less than 100 kHz in contrast to the usual 250kHz at (3 T). Therefore, diagnostics with lower acquisition frequency, such as the reflectometer, electron cyclotron emission and soft X-ray emission are all able to resolve Alfvén perturbations. The localisation and amplitude of Alfvén perturbations can be obtained from the soft X-ray horizontal camera and the microwave reflectometer measurements. Information about the localisation of the TAE fluctuations can also be obtained using external magnetic perturbations in NBI-heated plasmas with significant sheared toroidal rotation. The Doppler shift in the eigenmode frequencies combined with the information from the toroidal plasma rotation profile provides an additional estimate of the radial location of the AE.

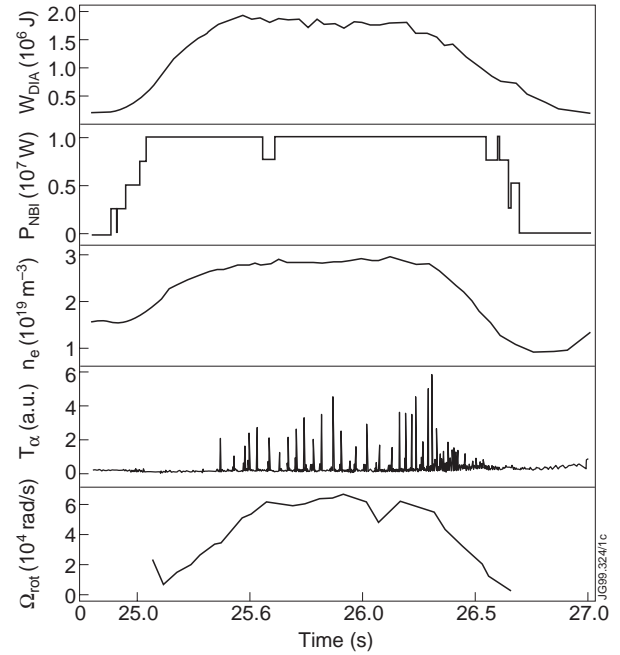


Fig.1. Overview of the plasma parameters in tritium discharge #43014 ($B_T = 0.9$ T, $I_p = 0.85$ MA, $n_T / (n_D + n_T) > 95\%$). Tritium NBI at $E_b = 160$ keV was kept constant at power 10 MW for 1.5 seconds. The T_α trace shows the signature of Edge Localized Modes (ELMs) in H-mode confinement regime. Toroidal plasma rotation Ω_{rot} is measured by charge-exchange spectroscopy.

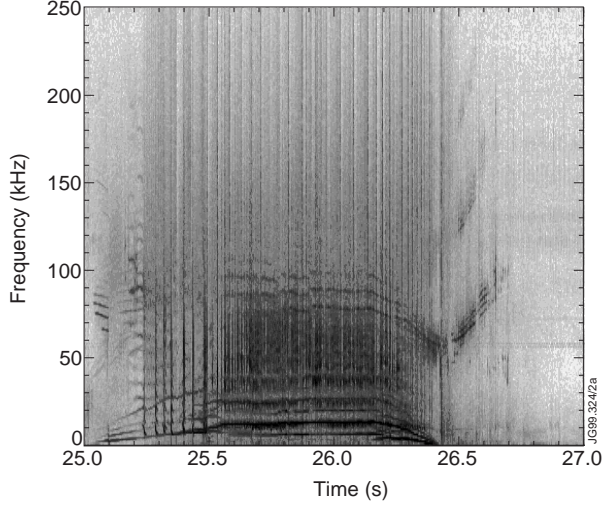


Fig.2a Overview of the Spectrum of the magnetic fluctuations for shot #43014 showing NBI driven AEs in JET. The magnetic fluctuations are dominated high beta related fluctuations such as strong fishbone activity. AEs are present throughout the NBI heated phase but they are clearer during the early phase (Figure 2b), when the bulk plasma beta is low. EAE modes are also visible with frequencies ranging from 130kHz to 150kHz.

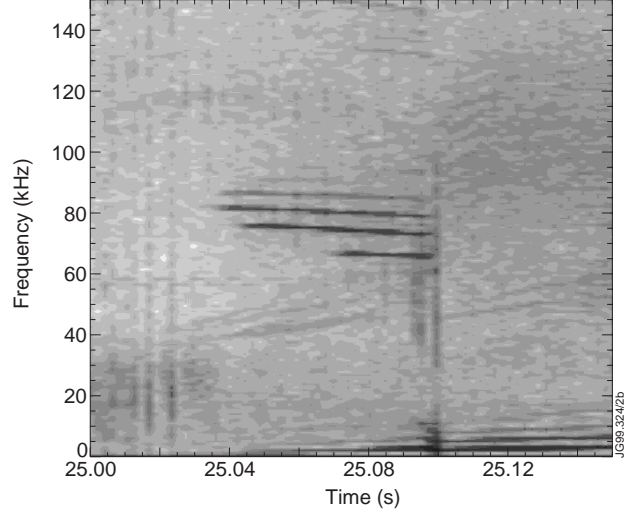


Fig.2b Spectrum of the magnetic fluctuations for shot #43014 showing NBI driven AEs in JET. The frequency range of the TAE activity is 70-90 kHz with the corresponding toroidal mode numbers ranging from $n=4,9$. The lower frequency fluctuations, with the frequency in the range of 0-10 kHz, are core instabilities with dominant toroidal mode number $n=1$.

The AE observed at low magnetic field, $B_T < 1$ T, have frequencies between 50-100 kHz (Figures 2a,2b), and intermediate toroidal mode numbers ($n=4-9$). The radial mode structure obtained using the horizontal soft X-ray camera shows that mode is of a global nature with highest amplitude displacements being localised outside the $q=1$ surface (Figure 3). The amplitude of the AE perturbations is small, of the order of $\frac{\delta B}{B} \approx 3 \times 10^{-5}$, as measured by the “Mirnov” coils.

The modelling of the Alfvén spectrum obtained using the CASTOR code [23,24,25] shows that the usual global ideal core localised TAE is close to the continuum and has very strong radiative damping. Calculations performed with both the non-ideal extension of the CASTOR code and the MISHKA-2 code [26] shows the existence of Kinetic Toroidicity Induced Alfvén Eigenmodes (KTAE) localised mainly in the gap just outside $q=1$ surface, consistent with the experimental observations. The continuum gap structure is shown in Figure 4 and the mode structure calculated by the

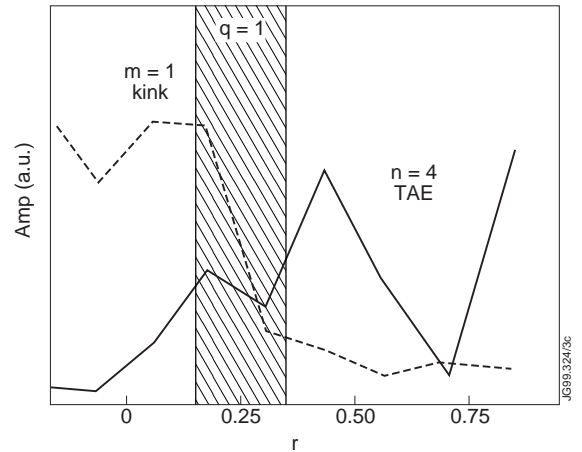


Fig.3 Radial mode structure of $n=4$ TAE mode and the $m=1$ internal kink determined by the SXR horizontal camera in the shot #43014. The radial localisation of the $n=1, m=1$ kink activity is used for a more accurate localisation of the $q=1$ surface. The AE measurement has poor resolution, but it is sufficient to conclude that the AE is global with the highest amplitude located outside the $q=1$ rational magnetic surface.

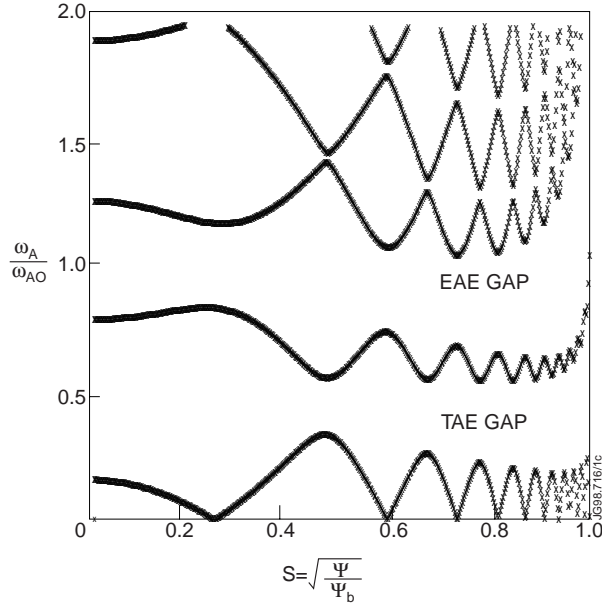


Fig. 4 shows the computed $n=4$ continuum gap structure for the shot #43014, $t=25.1s$ where TAE activity was observed. The toroidicity induced gap and the ellipticity induced gap are clearly visible.

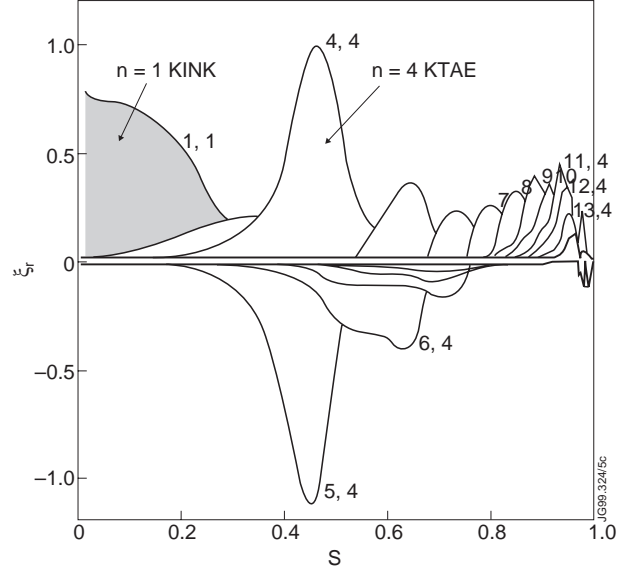


Fig.5 showing the $n=4$ AE mode structure for discharge #43014 and internal kink mode structure (shaded) computed by the CASTOR code. The radial structures of both the kink mode and the TAE are consistent with the experimental observations shown in figure 3.

CASTOR code is shown in Figure 5. The frequency of the $n=5$ AE computed by CASTOR is of $f_{AE(CASTOR)}=72.8$ kHz. This is close to the measured frequency $f_{AE(measured)}=75$ kHz. The plasma rotation frequency (f_{rot}) at the time of the comparison $t=25.1$ is small, of the order of $f_{rot(measured)}\sim 1-2$ kHz, where $f_{rot} = \Omega_{ROT}/2\pi$.

Direct information on the safety factor profile (q) can be obtained in discharges with known core MHD activity. A constraint on the safety factor profile is obtain from the localisation of the MHD fluctuations ($n=1, m=1$) associated with the rational surface $q=1$. The equilibrium reconstruction for the discharge #43014 is performed using the EFIT [27] code and HELENA [28] code with localisation of the $q=1$ surface consistent with radial extent of the $n=1 m=1$ core MHD activity shown in Figure 2b. Calculation of the Alfvén continuous spectrum is then performed by the CSCAS code [23] for the reconstructed equilibrium, see Figure 4.

3. MODELLING AND STABILITY THRESHOLDS

Unstable AE in the presence of fast particles require an efficient energy exchange between the energetic ions and the AE. The energy exchange between the eigenmodes and the energetic ions is maximised when the frequency of the modes is comparable with the frequency of the periodic motion of the orbits of the energetic ions. For NBI produced passing particles, the resonance condition is given approximately $V_{||} = V_A$ and the side band resonance condition $V_{||} = \frac{V_A}{3}$,

$$V_A = B_0 / \sqrt{4\pi \sum_i m_i n_i}, \text{ where } B_0 \text{ denotes the equilibrium magnetic field and } \sum_i m_i n_i \text{ is the}$$

plasma mass density. In addition, the balance of the wave-particle energy exchange must be favourable for instability. This is achieved when the ion diamagnetic drift frequency of the energetic ions exceeds the mode frequency ($\omega < n \omega_*$). If $\omega > n \omega_*$ the energetic ions provide a source of damping to the AE for non-inverted particle distributions $F(E) (\frac{dF}{dE} < 0)$ such as slowing down distributions.

In the case of destabilisation of AE with intermediate toroidal mode numbers ($4 < n < 10$) by moderate energy NBI ions ($E = < 160$ keV) the previous conditions can be met only for low values of the toroidal magnetic field ($B_T \sim 1$ T). Although for large toroidal mode numbers ($n > 10$) the condition ($\omega < n \omega_*$) can be satisfied at larger toroidal magnetic fields and larger densities, the damping of such AE is very high.

It was possible to estimate experimental thresholds for the beam-driven AE since the neutral beam power was increased slowly in the deuterium discharges and there were several shots in tritium discharges with different levels of beam power. The level of neutral beam power required to obtain instability was found to be of the order of 10 MW in tritium plasmas at 0.9 T and 8-10 MW in deuterium plasmas at 0.8 T. No AE activity was observed in hydrogen plasma discharges heated by hydrogen beams.

The modelling of the NBI drive on AE was performed using the CASTOR-K model [29,30]. The CASTOR-K code calculates the energy transfer between the AE and the energetic particles. Full orbit effects need to be retained since the beam ions have large orbits for magnetic fields of around 1 T and plasma currents of around 1 MA. The simulations are based on a plasma with electron density of $n_e = 2.5 \times 10^{19} \text{ m}^{-3}$ and slowing down distribution functions for the NBI ions where the measured ion temperature is of the order of $T_i = 3$ keV and the electron temperature is assumed to be ($T_i \sim T_e$). For the power level of $P_{NBI} = 10$ MW, which is the power threshold for destabilisation of AE, a NBI ion density on axis of $n_{beam} = 2.5 \times 10^{18} \text{ m}^{-3}$ was obtained from the deposition profile calculations (TRANSP). The radial deposition profile was best fitted by

$$n_{beam} \propto (1 - \bar{\psi})^2, \text{ where } \bar{\psi} \equiv \frac{\psi(r)}{\psi(r_{edge})}$$

and tritium plasmas with NBI injection with energies of 110 keV (hydrogen), 140 keV (deuterium) and 160 keV (tritium) were analysed. The calculations are based on the destabilisation of the $n=5$, which is the most unstable, with $f_{AE(CASTOR)} = 72.8$ kHz (with tritium) consistent with the experimental observations. In a deuterium plasma $f_{AE(CASTOR)} = 90$ kHz and in a hydrogen plasma $f_{AE(CASTOR)} = 128$ kHz. A strong drive $\gamma/\omega > 1\%$ from the deuterium and tritium beams was obtained for low values of magnetic field $B_T < 1$ T (Figure 6).

These simulations also show a larger drive from the tritium ions in comparison with the deuterium ions, which might explain the lower magnetic field ($B_T = 0.8$ T) required for the instability using deuterium NBI injection into deuterium plasma. Calculations of the damping of the mode considered, performed using the MISHKA-2 code, shows a strong damping rate of the

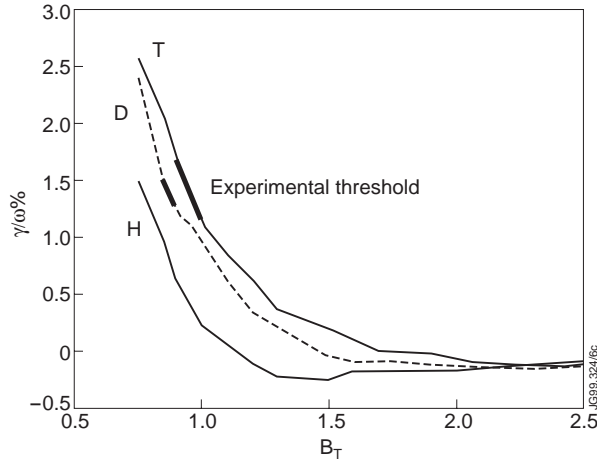


Fig.6 NBI drive as a function of the magnetic field for $n=5$ AE computed by the CASTOR-K code. The drive from NBI increases strongly with decreasing toroidal magnetic field. Results for hydrogen, deuterium and tritium plasmas with NBI injection with energies of 110 keV (hydrogen), 140 keV (deuterium) and 160 keV (tritium) are shown with a deposition beam ions profile fitted by $n_{BEAM} = 2.5 \times 10^{18} m^{-3} (1 - \psi)^2$

order of $\gamma/\omega \sim 1-2\%$. The CASTOR-K model shows that for the conditions where AE instability was observed experimentally, the drive provided by NBI is $\gamma/\omega > 1\%$. This result suggests that the drive from NBI has to overcome a strong damping of $\gamma/\omega \sim 1-2\%$ for instability, which is consistent with the strong damping calculated by the MISHKA-2 code and measured by the active AE excitation diagnostic at JET. These simulations also show that hydrogen beams had little or no drive on the AE considered for the parameters of the hydrogen experiments ($B_T=1$ T, $P_{NBI}=7$ MW), which is also consistent with the experimental observations. The destabilisation of the AE using hydrogen beams is expected for magnetic fields of the order $B_T < 0.7$ T with an NBI power of $P_{NBI}=10$ MW.

4. OBSERVATION OF HIGH AMPLITUDE FISHBONES

During the low toroidal magnetic field experiments in tritium plasmas, where AE activity was observed using NBI, the plasma volume averaged normalised beta was raised to

$$\beta_N = \frac{\beta}{(I_p/B_T a)} = 3.4, \text{ where, } I_p \text{ [MA] denotes the plasma current, } a \text{ [m] the minor radius and}$$

the toroidal magnetic field B_T [T]. In contrast to the AE activity, which was observed immediately after the beams have been switch on and with $\beta_N \approx 1.0$, the high amplitude fishbone appeared later with $\beta_N \approx 2.5$. Increasing number of fishbones with increasing amplitude are observed during the NBI heated phase. These modes have a dominant component $n=1$, but during the non-linear evolution several toroidal harmonics ($n=2-7$) are destabilised. The fishbone bursts are separated by approximately 25ms time intervals, which is comparable with the slowing down time of the NBI ions. The bursts last about 10ms and during this time the frequency of the $n=1$ perturbation

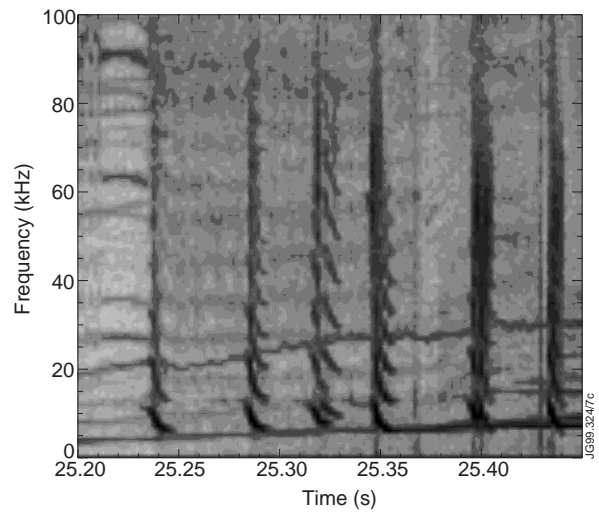


Fig.7 Spectrum of the magnetic fluctuations for shot 43014 showing fishbone bursts.

decreases from 15 kHz to 5 kHz in the laboratory reference frame, as shown in Figure 7. The amplitude of the fishbone bursts can be as high as $\frac{\delta B}{B} = 10^{-2}$, measured at the plasma edge. The fishbone mode structure measured by the soft X-ray camera shows that the mode is of a global nature, which is consistent with the mode structure of the internal kink perturbation at high beta with a large $q=1$ radius $r(q=1) \sim 0.5$. The plasma displacement measured by the soft X-rays emission during the fishbone mode is of the order of $0.01 m$.

5. FAST ION CONFINEMENT AND TRANSPORT

In contrast to what was reported in the DIII-D [7] and TFTR [10] experiments, no correlation was observed between neutron yield and AE activity in these discharges. The neutron yield in D-D plasmas is dominated by beam target reactions and in T-T plasmas by the beam reactions with the minority deuterium ions. Therefore, in D-D and T-T plasmas the fast ion losses can be estimated by the drops in the neutron yield. Drops of up to 10% in the neutron rate were observed during fishbone bursts in T-T (#43014), indicating beam losses during fishbone activity, see Figure 8. In hydrogen plasmas, the hydrogen beam does not produce neutrons, however, the confinement of the beam ions and losses can be estimated by transport analysis calculations.

In all these discharges, the discrepancy between the stored energy simulated by the transport code (TRANSP) and measured stored energy can be used to identify beam ion losses.

Detailed transport analysis performed using the TRANSP code did show a discrepancy, of up to 30%, between the simulated stored energy and the measured stored energy in the deuterium and tritium discharges where the AE and fishbones modes were observed, as shown in Figure 9.

This suggests that some redistribution of the energetic ions did occur during high power NBI injection in tritium and in deuterium, while good agreement was found for the hydrogen plasmas indicating no hydrogen beam losses. The most significant deviation was observed

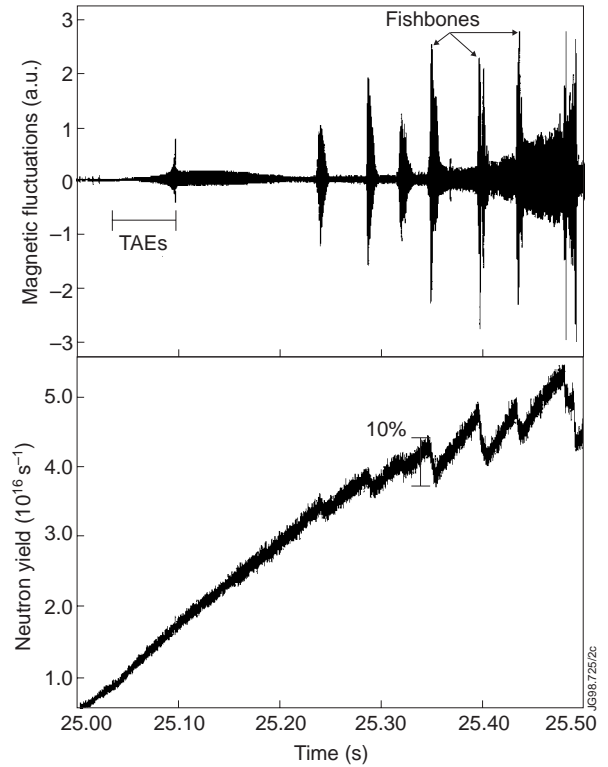


Fig.8 Time evolution of the magnetic fluctuations and the neutron yield in shot 43014 showing drops in the neutron yield of up to 10% during fishbones bursts. No effect on the neutron rate is observed during the appearance of AE at $t=25.05s$.

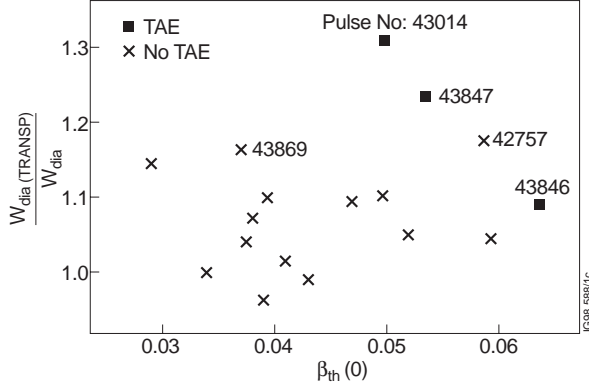


Fig.9 The deviation of the simulated stored energy and the measured stored ($W_{DIA(TRANSP)}/W_{DIA(MEASURED)}$) as computed by the TRANSP code as a function of the thermal plasma beta on axis, indicating where AE activity was observed.

during tritium injection into a tritium plasma (# 43014). In this discharge both AE and high amplitude fishbones were observed. The temporal evolution of the deviation between the measured stored energy and the calculated stored energy shown in the TRANSP calculations correlates with the observation of the high amplitude fishbones and no significant deviation is observed during AE activity, consistent with the neutron yield measurements.

CONCLUSIONS

AE destabilised by the injection of neutral beam ions were observed in JET at low toroidal magnetic fields ($B_T < 1T$). Unstable AE were observed in both deuterium and tritium plasmas, but were absent in hydrogen plasmas. The power threshold for the destabilisation of AE using a toroidal magnetic field of 0.8 T in deuterium and 0.9 T in tritium was $P_{NBI} = 8-10$ MW, which correspond to a beam density of $n_{beam} = 2.5 \times 10^{18} m^{-3}$. Detailed simulations performed using the CASTOR-K model showed that the drive $\gamma/\omega > 1\%$ provided by the neutral beam ions both in tritium (160 keV) and in deuterium (140 keV) for values of the magnetic field $B_T < 1T$ was sufficient to overcome the damping $\gamma/\omega \sim 1-2\%$ calculated by the MISHKA-2 code. No significant drive was provided by the 110 keV hydrogen beams for similar experimental conditions. These calculations predict that the destabilisation of AE using 110 keV would require magnetic fields of $B_T < 0.7 T$. The neutron rate showed no evidence of fast ion losses measured during AE activity. The TRANSP code shows a discrepancy between the simulated stored energy and the measured stored energy (of up to 30%) in the deuterium and tritium plasmas while no deviation was found in hydrogen plasmas. The temporal evolution of the deviation correlates with the observation of the fishbones, consistent with the observation of drops of up to 10% in the neutron emission during fishbone bursts.

In summary, the characterisation of AE instabilities in low magnetic field plasmas with intense NBI auxiliary heating completes the analysis of AE in D-T plasmas at JET. No evidence of fast ion losses and degradation of confinement was observed during the observation of AE in a very broad range of plasma conditions [8],[9],[16]. In particular, in low magnetic field plasmas, where the fast ion beta is maximised, the fast ion pressure is limited by the appearance of fishbone bursts and not by AE instabilities.

REFERENCES

- [1] ROSENBLUTH M.N., RUTHERFORD P.H., Phys. Rev. Lett. **34** (1975) 1428.
- [2] MIKHAILOVSKII A.B., Sov. Phys. JETP **41** (1975) 890.
- [3] CHENG, C.Z., CHEN, L., CHANCE, M.S., Ann. Physics **161** (1985) 21.
- [4] FU, G.Y., VAN DAM, J.W., Phys. Fluids **B1** (1989) 1949.
- [5] NAZIKIAN, R., et al., Phys. Rev. Lett. **78** (1997) 2976.
- [6] WONG, K.L., et al., Phys. Rev. Lett. **66** (1991) 1874.
- [7] HEIDBRINK W.W., STRAIT, E.J., DOYLE, E., SAGER, G., SNIDER, R., Nucl. Fusion **31** (1991) 1635.
- [8] FASOLI, A., et al., Plasma Phys. Control. Fusion **39** (1997) B287.
- [9] KERNER, W., et al., Nuclear Fusion **38** (1998) 1315.
- [10] DARROW, D.S., et al., Nucl. Fusion **37** (1997) 939.
- [11] FASOLI, A., et al., Nucl. Fusion **35** (1995) 1485.
- [12] FASOLI, A., et al., Nucl. Fusion **36** (1995) 258.
- [13] ALI-ARSHAD, S., CAMPBELL, D., Plasma Phys. Control. Fusion **37** (1995) 715.
- [14] WONG, K.L., et al., Plasma Phys. Control. Fusion **36** (1994) 879.
- [15] KIMURA, H., et al., Phys. Lett. A **199** (1995) 86.
- [16] SHARAPOV, S.E., et al., submitted to Nuclear Fusion (1998).
- [17] F. NAVE et al, Nuclear Fusion Vol. 31, (4) 1991, 697
- [18] T. KASS et al, 22nd EPS on Plasma Physics and Controlled Fusion, Bournemouth Part IV p41 1995
- [19] McGUIRE et al PRL 50,891, (1983)
- [20] B. COPPI et al Phys. Fluids 31, (6), June 1988, 1630
- [21] LIU CHEN et al 1984, PRL 52, 13, March 1984, 1122
- [22] T. HENDER, Theory of Fusion Plasmas, Varrena (1998)
- [23] S. POETDS et al JCP Vol. 105, 1, March 1993, 165
- [24] G.T.A. HUYSMANS et al, Phys. Fluids B5, 1545, (1993)
- [25] W. KERNER et al, JCP 142, p271, 1998
- [26] MIKHAILOVSKII, A.B., HUYSMANS, G.T.A., KERNER, W., SHARAPOV, S.E., Plasma Physics Reports **23** (1997) 844.
- [27] O'BRIEN, D., et al., Nucl. Fusion **32** (1992) 1351.
- [28] HUYSMANS, G.T.A., GOEDBLOED, J.P., KERNER, W., in Proceed. CP90 Conf. on Comput. Physics, World Scientific Publ. Co. (1991), p.371.
- [29] BORBA, D., CANDY, J., KERNER, W., SHARAPOV, S., in: Theory of Fusion Plasmas, ed. J.W.Connor, E.Sindoni and J.Vaclavik (Societa Italiana di Fisica/Editrice Compositori, Bologna, 1996), p.267.
- [30] D. BORBA and W. KERNER, submitted to JCP

